CORRESPONDENCE

Dynamic Contrast-enhanced MRI Demonstrates Pulmonary Microvascular Abnormalities Months After SARS-CoV-2 Infection

Iris Y. Zhou[1,2,3]*, Molly Mascia[1,4]*, George A. Alba[1,4],
Michael Magaletta[2], Leo C. Ginns[1,4], Peter Caravan[1,2,3], and
Sydney B. Montesi[1,3,4]

[1]Harvard Medical School, Boston, Massachusetts; and [2]Athinoula
A. Martinos Center for Biomedical Imaging, Department of Radiology,
[3]Institute for Innovation in Imaging, and [4]Division of Pulmonary and Critical
Care Medicine, Massachusetts General Hospital, Boston, Massachusetts

ORCID IDs: 0000-0002-4351-7398 (I.Y.Z.); 0000-0002-6876-7836
(G.A.A.).

To the Editor:

Severe acute respiratory syndrome coronavirus 2 (SARS-CoV-2) causes vascular endothelial abnormalities (1). Pulmonary vascular dysfunction is a key component of severe SARS-CoV-2 infection (2). The extent of endothelial dysfunction in nonsevere infection and its sequelae are not fully understood. We and others recently showed that dynamic contrast-enhanced magnetic resonance imaging (DCE-MRI) could detect microvascular differences in patients with idiopathic pulmonary fibrosis (IPF) compared with healthy volunteers (3, 4). DCE-MRI involves continuous dynamic imaging before, during, and after injection of gadolinium-based contrast. The resultant signal intensity versus time curve provides information regarding microvascular perfusion and extravascular extracellular space (5). We hypothesized that DCE-MRI could detect microvascular changes in individuals with prior symptomatic SARS-CoV-2 infection.

Some study results have been reported in abstract format (6).

This study was approved by the Massachusetts General Brigham Institutional Review Board. All participants provided written informed consent. Individuals with prior coronavirus disease (COVID-19) who had a positive SARS-CoV-2 PCR test within the previous 3–12 months were recruited through the Massachusetts General Hospital Coronavirus Recovery Clinic. Healthy volunteers without known lung disease were recruited through a different protocol. Participants were excluded for respiratory illness within the past 6 weeks, cigarette smoking within the past 6 months, gadolinium allergy, or contraindications to MRI.

DCE-MRI was performed using a 3T MRI scanner (Siemens Healthineers) using a radial sampling sequence: flip angle, 15°; echo time, 1.0 ms; repetition time, 3.4 ms; field of view, 410 × 410 mm^2;

*Co–first authors.

voxel size, 2.1 × 2.1 × 2.5 mm^3; and 72 slices. Serial volumetric pulmonary images were acquired during free breathing and reconstructed to a temporal resolution of 2.75 seconds (7–10). Imaging acquisition started 60 seconds before injection of 0.05 mmol/ kg gadoterate meglumine (Guerbet) at a rate of 4 ml/s and continued for 360 seconds. Signal intensity versus time curve was extracted for the entire lungs and for a region of interest (ROI) from a posterior coronal plane which included the lungs but excluded large vessels. We measured the magnitude of peak enhancement, the rate of contrast arrival (k_{washin}), time to peak enhancement, the full width at half maximum for the peak (FWHM) as a surrogate of contrast transit time, and the rate of contrast washout ($k_{washout}$), as defined previously (3). Prior COVID-19 participants completed the modified Medical Research Council (mMRC) dyspnea scale. Hospitalization status, pulmonary function testing (PFT), and chest computed tomography (CT) results were recorded from the medical record. Differences between groups were assessed using the Wilcoxon rank-sum test or Fisher's exact test, with $P < 0.05$ considered statistically significant. Spearman's rank correlation coefficient was used to assess the relationship between time from positive SARS-CoV-2 PCR test and MRI measurements.

Ten participants with prior COVID-19 (median age, 57 years; 50% male) and 10 healthy volunteers (median age, 43 years; 40% male) underwent DCE-MRI (Table 1). For participants with prior COVID-19, the average time from positive SARS-CoV-2 PCR test to DCE-MRI was 7.8 months. Positive SARS-CoV-2 PCR tests occurred between September 2020 and September 2021. Three participants required hospitalization for COVID-19, two of whom required supplemental oxygen (maximum flow rate, 4 L/min). Median mMRC score on the day of DCE-MRI was 1 (range = 0–2). All underwent clinically obtained spirometry, lung volumes, and $D_{L_{CO}}$, and 5 had chest CT imaging performed after COVID-19 and before DCE-MRI. Two participants had mild restriction, with 1 having a mild diffusion impairment. One participant had borderline mild obstruction. Remaining PFT results were normal. Of the participants that had chest CT imaging, 3 had no parenchymal abnormalities, and 2 had minimal residual parenchymal abnormalities.

Group averaged signal versus time curves obtained from a posterior coronal ROI are shown in Figure 1A. Compared with healthy volunteers, participants with prior COVID-19 had signal versus time curves that were consistent with reduced pulmonary microvascular perfusion: The rate of contrast arrival to tissue (k_{washin}) was significantly slower (1,900%/min vs. 2,400%/min), the peak itself was significantly broader (FWHM, 0.17 min vs. 0.14 min), and there was a trend toward a lower magnitude of peak enhancement (210% vs. 250%) (Table 1). Unlike in IPF participants, for whom the rate of contrast washout was significantly slower than for healthy volunteers (3), in this study, participants with prior COVID-19 showed no differences in $k_{washout}$ between groups (−5.6%/min vs. −6.10%/min), and this suggests that there is no extravascular extracellular volume expansion occurring in the participants with prior COVID-19. There was a trend toward a slower k_{washin} in the analysis of the entire lungs (1,500%/min vs. 1,800%/min), although no microvascular parameters reached significance, indicating that the effect might be posterior predominant. Parametric maps of a posterior coronal ROI for a participant with prior COVID-19 demonstrate that measurements of microvascular perfusion are diffusely reduced throughout the lungs compared with those for a healthy volunteer (Figure 1B). There was a

Table 1. Descriptive Statistics by Participants with Prior Coronavirus Disease versus Healthy Volunteer Groups

Variable	Participants with Prior COVID-19 ($n = 10$)	Healthy Volunteers ($n = 10$)	P Value
Age, median (range)	57 (37–76)	43 (27–74)	0.42*
Male, frequency (%)	5 (50)	4 (40)	>0.99[†]
mMRC, median (range)	1 (0–2)[‡]	—	—
Hospitalization for COVID-19, frequency (%)	3 (30)	—	—
Mechanical ventilation, frequency (%)	0 (0)	—	—
Noninvasive ventilation, frequency (%)	0 (0)	—	—
Supplemental oxygen, frequency (%)	2 (20)	—	—
FEV_1,% predicted, mean ± SD	96.5 ± 15.2	—	—
FVC, % predicted, mean ± SD	98.6 ± 14.5	—	—
FEV_1/FVC, mean ± SD	76.9 ± 4.6	—	—
$D_{L_{CO}}$, % predicted, mean ± SD	99.4 ± 15.0	—	—
TLC, % predicted, mean ± SD	86.7 ± 14.2	—	—
Peak enhancement, %, median (range)			
Posterior coronal	210 (90–270)	250 (200–410)	0.06*
Whole lung	170 (80–250)	200 (160–340)	0.12*
TTP, min, median (range)			
Posterior coronal	0.12 (0.10–0.17)	0.11 (0.09–0.12)	0.25*
Whole lung	0.12 (0.10–0.16)	0.12 (0.11–0.13)	0.67*
k_{washin}, %/min, median (range)			
Posterior coronal	1,900 (770–2,800)	2,400 (1,900–3,400)	0.04*
Whole lung	1,500 (770–2,200)	1,800 (1,500–2,600)	0.09*
FWHM, min, median (range)			
Posterior coronal	0.17 (0.11–0.38)	0.14 (0.11–0.15)	0.02*
Whole lung	0.17 (0.12–0.28)	0.15 (0.12–0.18)	0.44*
$k_{washout}$, %/min, median (range)			
Posterior coronal	−5.60 (−10.50 to −2.10)	−6.10 (−13.30 to −3.40)	0.53*
Whole lung	−4.10 (−6.70 to −0.50)	−4.60 (−8.20 to −1.20)	0.58*

Definition of abbreviations: COVID-19 = coronavirus disease; FWHM = full width at half maximum; k_{washin} = rate of contrast arrival; $k_{washout}$ = rate of contrast washout; mMRC = modified Medical Research Council dyspnea scale; TTP = time to peak enhancement.
Data are reported as mean ± SD, frequency (percentage), or median (range).
*Wilcoxon rank-sum test.
[†]Fisher's exact test.
[‡]mMRC results performed at the time of MRI and were only available for 9 participants.

positive correlation between the time between positive SARS CoV-2 PCR testing and MRI and peak enhancement from the posterior lung (Spearman $r = 0.66$, $P = 0.04$) but not with k_{washin} or FWHM.

Our study has several important findings. First, in a small group of participants with remote and predominantly nonsevere COVID-19, pulmonary microvascular perfusion was reduced compared with age-similar healthy volunteers. Notably, 90% of the participants with prior COVID-19 had normal $D_{L_{CO}}$ values, suggesting that DCE-MRI is more sensitive to detecting microvascular abnormalities. Second, rates of contrast washout were similar between groups, arguing against significant residual tissue fibrosis or edema.

There is growing interest in using functional lung imaging to assess postacute sequelae of SARS-CoV-2 infection. Yu and colleagues performed DCE-MRI in individuals with persistent dyspnea after COVID-19 and demonstrated a late bolus arrival of contrast compared with healthy volunteers (11). However, in that study, DCE-MRI was performed during a single breathhold (40 s), preventing extravascular extracellular space information from being obtained. Only perfusion parameters related to time to peak enhancement were analyzed. Grist and colleagues performed

hyperpolarized ^{129}Xe MRI in participants with breathlessness, despite normal to near-normal chest CT imaging at least 3 months after hospital discharge for COVID-19 and demonstrated reduced alveolar-capillary diffusion compared with healthy volunteers (12). Our results build on these findings and further demonstrate the sensitivity of DCE-MRI for detecting pulmonary microvascular pathology.

We are unable to draw associations with the DCE-MRI–derived measurements and CT findings, PFT abnormalities, or persistent dyspnea given our sample size. Although our results demonstrate the sensitivity of DCE-MRI for assessing microvascular differences, our small sample size may have prevented us from detecting other differences or correlations. For example, the variability in $k_{washout}$ may mask possible changes in extracellular volume in a subset of subjects. Similarly, we observed a positive correlation with peak enhancement versus time from positive PCR, but this was not observed with k_{washin} or FWHM. Our results included participants who had COVID-19 before the emergence of the omicron variant. It is plausible that different strains of SARS-CoV-2 have different predilections for causing pulmonary vascular dysfunction. We cannot
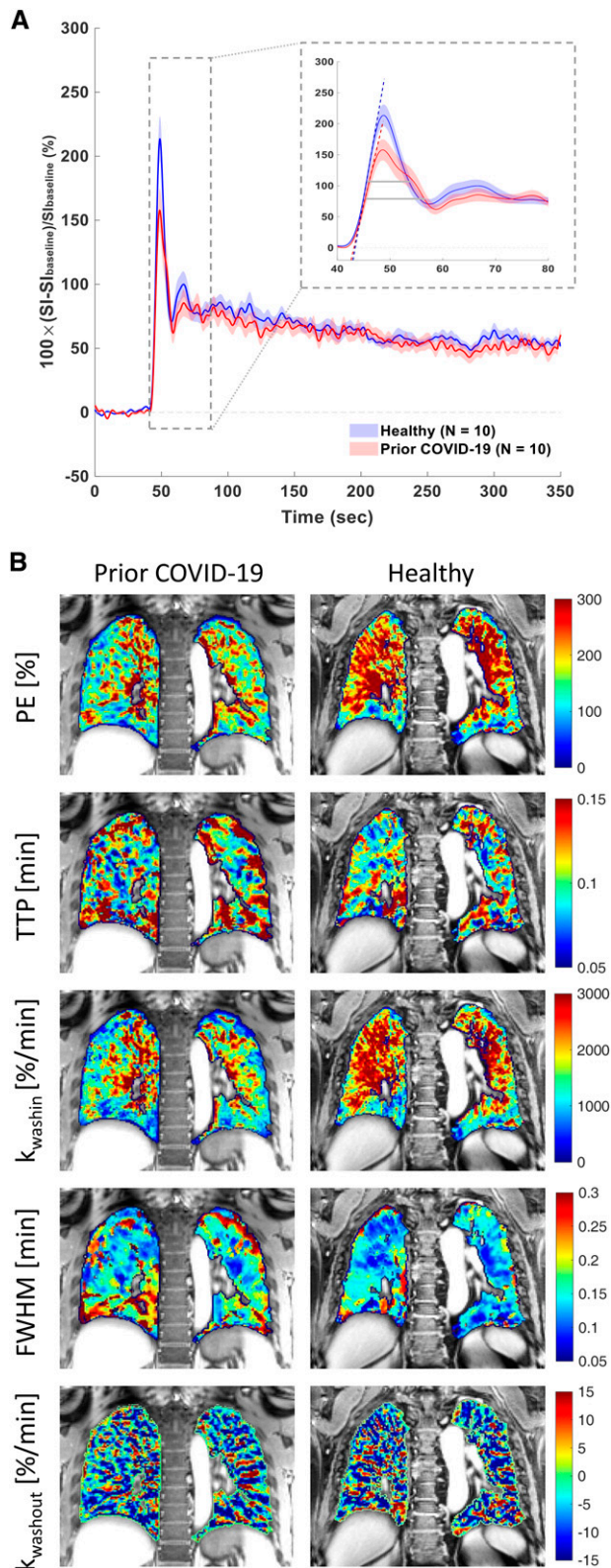
Figure 1. Dynamic contrast-enhanced magnetic resonance imaging of prior coronavirus disease participants versus healthy volunteers. (*A*) Magnetic resonance imaging signal intensity (SI) versus time curves of the lung parenchyma from healthy volunteers (*n* = 10) and

confirm the absence of prior SARS-CoV-2 infection in the healthy volunteers. We acknowledge the potential for selection bias in the recruitment of participants with prior SARS-CoV-2 infection as the degree of symptomatology could have influenced referral to our Coronavirus Recovery Clinic.

Our results support microvascular perfusion abnormalities months after COVID-19. The driver of these findings, such as residual microvascular thrombosis or sequelae of vascular remodeling, remains to be determined (13, 14). Understanding the pathophysiologic underpinnings of our findings may have therapeutic relevance for acute SARS-CoV-2 infection and postacute sequelae of SARS-CoV-2 infection. ∎

Correspondence and requests for reprints should be addressed to Sydney B. Montesi, M.D., Massachusetts General Hospital, 55 Fruit Street, BUL-148, Boston, MA 02114. Email: sbmontesi@partners.org.

References

1. Siddiqi HK, Libby P, Ridker PM. COVID-19—a vascular disease. *Trends Cardiovasc Med* 2021;31:1–5.
2. Patel BV, Arachchillage DJ, Ridge CA, Bianchi P, Doyle JF, Garfield B, *et al.* Pulmonary angiopathy in severe COVID-19: physiologic, imaging, and hematologic observations. *Am J Respir Crit Care Med* 2020;202: 690–699.
3. Montesi SB, Zhou IY, Liang LL, Digumarthy SR, Mercaldo S, Mercaldo N, *et al.* Dynamic contrast-enhanced magnetic resonance imaging of the lung reveals important pathobiology in idiopathic pulmonary fibrosis. *ERJ Open Res* 2021;7:00907–02020.
4. Weatherley ND, Eaden JA, Hughes PJC, Austin M, Smith L, Bray J, *et al.* Quantification of pulmonary perfusion in idiopathic pulmonary fibrosis with first pass dynamic contrast-enhanced perfusion MRI. *Thorax* 2021; 76:144–151.
5. Cuenod CA, Balvay D. Perfusion and vascular permeability: basic concepts and measurement in DCE-CT and DCE-MRI. *Diagn Interv Imaging* 2013;94:1187–1204.
6. Montesi SB, Mascia M, Alba GA, Magaletta M, Caravan P, Zhou I, *et al.* Dynamic contrast-enhanced lung MRI in COVID-19 survivors may demonstrate ongoing microvascular abnormalities [abstract]. *Am J Respir Crit Care Med* 2022;205:A3906.

Figure 1. (*Continued*). participants with prior coronavirus disease (COVID-19) (*n* = 10) computed as percentage of SI change relative to the lung signal before gadolinium administration. The group-averaged dynamic curves from posterior coronal regions of interest are shown. Shaded area indicates mean ± 1 SEM. The inset shows the zoom-in of the first-pass peaks, with dashed lines indicating the upslopes and gray horizontal bars indicating the full width at half maximum (FWHM) of the first-pass peaks. (*B*) Representative parametric maps of peak enhancement, TTP, k_{washin}, FWHM, and $k_{washout}$ from a posterior coronal region of interest of a participant who had prior COVID-19 and who did not require hospitalization and a healthy volunteer. k_{washin} = rate of contrast washin; $k_{washout}$ = late-phase washout slope between 60 seconds postinjection and the last acquisition; PE = peak enhancement; TTP = time to peak enhancement.

7. Block KT, Chandarana H, Milla S, Bruno M, Mulholland T, Fatterpekar G, *et al.* Towards routine clinical use of radial stack-of-stars 3D gradient-echo sequences for reducing motion sensitivity. *J Korean Soc Magnetic Reson Med* 2014;18:87–106.

8. Chandarana H, Block TK, Ream J, Mikheev A, Sigal SH, Otazo R, *et al.* Estimating liver perfusion from free-breathing continuously acquired dynamic gadolinium-ethoxybenzyl-diethylenetriamine pentaacetic acid–enhanced acquisition with compressed sensing reconstruction. *Invest Radiol* 2015;50:88–94.

9. Kumar S, Rai R, Stemmer A, Josan S, Holloway L, Vinod S, *et al.* Feasibility of free breathing lung MRI for radiotherapy using non-Cartesian k-space acquisition schemes. *Br J Radiol* 2017;90:20170037.

10. Frenk NE, Montesi SB, Chen T, Liang LL, Zhou I, Seethamraju R, *et al.* Free-breathing dynamic contrast-enhanced magnetic resonance of interstitial lung fibrosis. *Magn Reson Imaging* 2020;69:16–21.

11. Yu JZ, Granberg T, Shams R, Petersson S, Sköld M, Nyrén S, *et al.* Lung perfusion disturbances in nonhospitalized post-COVID with dyspnea-A magnetic resonance imaging feasibility study. *J Intern Med* 2022;292:941–956.

12. Grist JT, Chen M, Collier GJ, Raman B, Abueid G, McIntyre A, *et al.* Hyperpolarized ^{129}Xe MRI abnormalities in dyspneic patients 3 months after COVID-19 pneumonia: preliminary results. *Radiology* 2021;301: E353–E360.

13. Grillet F, Busse-Coté A, Calame P, Behr J, Delabrousse E, Aubry S. COVID-19 pneumonia: microvascular disease revealed on pulmonary dual-energy computed tomography angiography. *Quant Imaging Med Surg* 2020;10:1852–1862.

14. Ackermann M, Tafforeau P, Wagner WL, Walsh CL, Werlein C, Kühnel MP, *et al.* The bronchial circulation in COVID-19 pneumonia. *Am J Respir Crit Care Med* 2022;205:121–125.

Check for updates

Applying Intersectionality to Better Characterize Healthcare Disparities for Critically Ill Adults

Gwenyth L. Day[1], Edward P. Havranek[3,4], Eric G. Campbell[3], and Anuj B. Mehta[1,4]

[1]Division of Pulmonary Medicine and Critical Care Sciences, [2]Division of Cardiology, and [3]Division of General Internal Medicine, University of Colorado, Aurora, Colorado; and [4]Department of Medicine, Denver Health & Hospital Authority, Denver, Colorado

ORCID IDs: 0000-0002-7426-5744 (G.L.D.); 0000-0002-8022-2492 (E.G.C.); 0000-0002-8993-6803 (A.B.M.).

To the Editor:

It remains unclear whether patients of different sexes or races experience disparate outcomes after mechanical ventilation (MV).

Although some studies initially identified racial differences in acute respiratory failure outcomes, many of these differences abated after controlling for age, severity of illness, and comorbidities (1–3). However, there is observational evidence for sex- and race-based differences in critical care. Patients identified as female or non-White with acute respiratory distress syndrome are less likely to receive low-tidal volume ventilation, and patients identified as Black are more likely to experience occult hypoxemia (4–6). Studies that evaluated the effect of race, sex, or ethnicity as single exposures may dilute the interactive effect of multiple social determinants on healthcare delivery and outcomes, potentially masking relevant disparities. Intersectionality is a conceptual framework and approach that aims to understand how multiple identities interact to produce variable experiences of privilege and vulnerability (7). The principal assertion is that outcomes organized by intersectional identity may better approximate the health-related experience of the individual shaped by common social processes (8). On a conceptual level, organization around intersectional variables emphasizes the experience of patients in that group as distinct. For example, the experiences of a patient identified as female and Black are unique and not a summation of the experiences of a patient identified as Black plus the experiences of a patient identified as female. We evaluated the intersectional effect of race and sex to identify subgroups of patients with increased vulnerability to in-hospital death after MV for pneumonia or sepsis to better characterize potential healthcare disparities in the ICU.

Methods

We conducted a retrospective cohort study using seven geographically and racially diverse state inpatient databases (Arizona, California, Florida, Iowa, Maryland, Mississippi, and New York) from 2018 to 2019, identifying adult nonsurgical patients treated with MV with pneumonia or sepsis on admission with discharge billing codes (9, 10). An eight-category intersectional variable based on race and sex was created (male White, male Black, male Asian, male Other, female White, female Black, female Asian, female Other).

To determine if an intersectional approach identified greater variability, we determined hospital mortality on the basis of sex, race, and intersectional identity separately. We determined risk-adjusted mortality in two ways. In three separate models, we used hierarchical logistic regression with each demographic category (sex, race, and intersectional identity) as a random intercept to calculate risk-adjusted mortality percentages. In the second approach, demographic categories (sex, race, and intersectional identity) were treated as fixed effects in three separate hierarchical regression models with the hospital as a random intercept to determine the adjusted odds ratio for death. Models were adjusted for patient age, 38 individual Elixhauser comorbidities, and acute organ failures present on admission (11).

Results

We identified 161,560 adult nonsurgical patients with pneumonia or sepsis who received MV. Patients identified as female or Asian were the oldest groups, whereas patients identified as Other race were the youngest (Table 1). In general, patients identified as male, Black, or Asian were more acutely and chronically ill. After risk adjustment, no significant difference in risk-adjusted mortality rates was observed on the basis of sex or race alone, although male patients had slightly